BODIPY-based conjugated microporous polymers as reusable heterogeneous photosensitisers in a photochemical flow reactor

Polymer Chemistry

Accepted Manuscript

This article can be cited before page numbers have been issued, to do this please use: J. M. Tobin, J. Liu, H. Hayes, M. Demleitner, D. Ellis, V. Arrighi, Z. Xu and F. Vilela, *Polym. Chem.*, 2016, DOI: 10.1039/C6PY01393G.

This is an *Accepted Manuscript*, which has been through the Royal Society of Chemistry peer review process and has been accepted for publication.

Accepted Manuscripts are published online shortly after acceptance, before technical editing, formatting and proof reading. Using this free service, authors can make their results available to the community, in citable form, before we publish the edited article. We will replace this *Accepted Manuscript* with the edited and formatted *Advance Article* as soon as it is available.

You can find more information about *Accepted Manuscripts* in the Information for Authors.

Please note that technical editing may introduce minor changes to the text and/or graphics, which may alter content. The journal's standard Terms & Conditions and the Ethical guidelines still apply. In no event shall the Royal Society of Chemistry be held responsible for any errors or omissions in this *Accepted Manuscript* or any consequences arising from the use of any information it contains.

ROYAL SOCIETY OF CHEMISTRY

www.rsc.org/polymers

View Article Online
DOI: 10.1039/C6PY01393G

Journal Name

ARTICLE

BODIPY-based conjugated microporous polymers as reusable heterogeneous photosensitisers in a photochemical flow reactor

Received 00th January 20xx,
Accepted 00th January 20xx

DOI: 10.1039/x0xx00000x

www.rsc.org/

J. M. Tobin,[†,a] J. Liu,[†,b] H. Hayes,[a] M. Demleitner,[a] D. Ellis,[a] V. Arrighi,[a] Z. Xu,*[,b] F. Vilela*[,a]

BODIPY-based conjugated microporous polymers (BDP_CMP and PHTT_BDP) have been synthesised via two distinct methods of assembly: high-yielding Suzuki-Miyaura cross-coupling of BODIPY-containing building blocks, and post-synthetic conversion of an aldehyde-equipped CMP host that was synthesised in the absence of metal-based catalysts. Both approaches yielded BODIPY-based materials featuring high BET surface area (484-769 m^2 g^{-1}) and a bathochromic shift in the maximum light absorbance (520-550 nm). Singlet oxygen production employing the BODIPY-based materials at 530 nm was carried out heterogeneously in a commercial photochemical flow reactor.

Introduction

Anthropogenic climate change as a result of our current energy demands is of great concern in today's society. The need for new sources of clean and renewable energy alongside with improved sustainable chemical processes has been the driving force behind the development of many new materials. One class of materials that has recently gained a great deal of attention from the research community consist of systems with inherent porosity.[1] These materials have the potential to provide a means to store and separate chemical entities such as gases;[2] participate in (photo)catalytic processes such as hydrogen evolution from water;[3] and in the storage and delivery of energy.[4] Conjugated microporous polymers (CMPs) fall into this class of materials.

As first described by Cooper *et al.*,[5,6] CMPs have been investigated as counterparts to zeolites, metal-organic frameworks, covalent-organic frameworks and other microporous polymers.[7] Combining high surface areas, microporosity and photoactivity, CMPs have also shown applications in gas sorption and separation,[8] light harvesting,[9] and heterogeneous (photo)catalysis,[10-13] amongst others. One important application where CMPs have recently gained traction is in the heterogeneous photoactivation of singlet oxygen ($^1O_2$).[11,14,15]

Unlike most natural compounds, molecular oxygen has triplet multiplicity ($^3O_2$) in the ground state and two excited singlet states.[16] The most common and widely used generation of $^1O_2$ is based on homogenous photosensitisers.[17,18] This simple method requires only an oxygen source, light of an appropriate wavelength and a photosensitiser possessing an energetically suitable excited triplet state. Through the absorption of light, the photosensitiser is excited to its singlet state and *via* a subsequent intersystem crossing mechanism it populates into a triplet state. The excited sensitiser can then transfer energy and spin to the ground state $^3O_2$, thus forming the excited $^1O_2$.[18] Given its strong electrophilic and oxidising character, it has been widely used as a versatile synthetic reagent in a range of applications including organic synthesis,[19] environmental water treatment[20] or photodynamic therapy of cancer.[21]

One particular dye that is effective in the production of singlet oxygen is BODIPY (4,4-difluoro-4-bora-3a,4a-diaza-s-indacene), Fig. 1.[22] Due to its strong absorption–emission and fluorescence properties, as well as chemical robustness,[23-25] BODIPY derivatives have also been widely employed for different applications such as biological tags with visible to near-IR emission, molecular rotors, lasing, dye-sensitised solar cells, electroluminescence and chemical photosensitisation reactions.[25-35] This strong electron-accepting dye has therefore the necessary properties for photosensitisation at higher wavelengths of $^1O_2$ when incorporated into a CMP.

As part of our ongoing efforts to develop versatile synthetic strategies for functional CMP solids, herein we report the chemical synthesis and characterisation of two novel BODIPY-based CMPs, which exhibits high surface areas and a bathochromic shift with their maximum light absorbance at 520-550 nm. These polymers were tested in a commercial photochemical flow reactor[36] for the production of $^1O_2$ in multiple solvents, and simply using air as the source of oxygen.

[a] School of Engineering and Physical Sciences, Heriot-Watt University, Edinburgh, EH14 4AS, United Kingdom. E-mail: F.Vilela@hw.ac.uk
[b] Department of Biology and Chemistry, City University of Hong Kong,83 Tat Chee Avenue, Kowloon, Hong Kong SAR. E-mail: zhengtao@cityu.edu.uk
† These authors contributed equally to this work.
Electronic Supplementary Information (ESI) available: NMR data, solid state UV-visible spectra, FT-IR spectra, TGA traces, N_2 and CO_2 sorption isotherms, SEM and TEM images, EDX spectra. See DOI: 10.1039/x0xx00000x

View Article Online
DOI: 10.1039/C6PY01393G

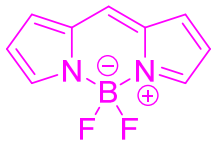

Fig. 1 Chemical structure of the BODIPY core.

The BODIPY-based CMPs prove to be efficient photosensitisers under the conditions tested and can be easily recovered and isolated *via* simple filtration and then conveniently reused multiple times. Furthermore, in photocatalytic reactions, a photosensitiser that absorbs light at higher wavelengths is desirable as it mitigates photodecomposition of staring materials and/or products whilst also avoiding undesirable side reactions when more energetic light sources such as UV are employed.

Experimental

Instrumentation and Measurements

All reagents and starting materials employed in this work were commercially available and used without further purification unless otherwise stated. ^{1}H NMR and ^{13}C NMR were recorded on a 400 MHz Bruker superconducting-magnet high-field NMR spectrometer at room temperature with tetramethylsilane as the internal standard or a 300 MHz Bruker AV-III300 spectrometer at room temperature. Solid state ^{13}C NMR CP-MAS measurements were carried out using a Bruker Advance 400 spectrometer operating at 100.6 MHz for ^{13}C using a Bruker 4 mm double resonance probe-head operating at a spinning rate of 10-12.5 kHz. Solution UV-Vis spectra were recorded on a PerkinElmer Lambda 25 system using 10 mm quartz cuvettes with CH_2Cl_2 as the solvent. Solid-state UV-Vis spectra were recorded on the same system using a Labsphere RSA-PE-20 reflectance spectroscopy integration sphere. Fluorescence spectra were recorded on a Perkin Elmer LS 55 spectrometer using 10 mm quartz fluorescence cell with CH_2Cl_2 as the solvent. FT-IR spectra were recorded on a Nicolet Avatar 360 FT-IR spectrophotometer or an ATR-FTIR spectrometer *Thermo Scientific Nicolet iS5*. Thermogravimetric analysis (TGA) of the BDP_CMP sample was carried out in a nitrogen stream using TA Instruments Q50 Thermogravimetric Analyser with a heating rate of 3 °C min^{-1} and a heating range of 30 °C to 950 °C. TGA of the PHTT_BDP sample was carried out in a nitrogen stream using PerkinElmer Thermal analysis equipment (STA 6000) with a heating rate of 3 °C min^{-1}, with an empty Al_2O_3 crucible being used as the reference. BET Surface area was carried out using a Quantachrome Autosorb iQ gas sorption analyser. Each sample was outgassed at 0.03 torr with a 2 °C min^{-1} ramp to 100 °C and held at 100 °C for 12 hours. The sample was then held at vacuum until the analysis was run. Pore analysis was performed using N_2 at 77 K (P/P_0 range of 1×10^{-5} to 0.995) and CO_2 at 273 K (P range of 8×10^{-3} to 780 mmHg). Scanning electron microscopy (SEM) was carried out on Philips XL30 Esem-FEG, (FEI Company, The Netherlands) equipped with an energy-dispersive x-ray microanalysis (EDX) system (EDAX Phoenix system, EDAX Inc., Mahwah NJ, USA). Transmission electronic microscopy (TEM) was conducted on a Philips Technai 12 Transmission Electron Microscope with an accelerating voltage of 120 KV.

Syntheses

Two distinct synthetic strategies were examined. First, in a direct assembly approach, BDP_CMP was obtained using a palladium-catalysed Suzuki-Miyaura cross-coupling reaction, whereby 1,3,5-tris(4,4,5,5-tetramethyl-1,3,2-dioxaborolan-2-yl)benzene was used as the cross-linker reacting with 2,6-dibromo-1,3,5,7-tetramethyl-8-phenyl-BODIPY monomer (Scheme 1). Tetrakis(triphenylphosphine) palladium(0), 1,3,5-tris(4,4,5,5-tetramethyl-1,3,2-dioxaborolan-2-yl)benzene and 2,6-dibromo-1,3,5,7-tetramethyl-8-phenyl-BODIPY were synthesised *via* literature methods[37-40] which can be found in the ESI. A monomeric version of the repeat unit, 2,6-diphenyl-1,3,5,7-tetramethyl-8-phenyl-BODIPY (BDP_Ph), was also synthesised through a similar cross-coupling reaction and compared to results found in literature.[41] The scheme and structure for BDP_Ph is presented in the ESI. Second, in a post-synthetic functionalisation approach, the aldehyde groups of a known polymer system PHTT_CHO, as described in our previous work,[13] were converted into the BODIPY function *via* the classical protocol of condensation with 2,4-dimethylpyrrole, followed by oxidation via 2,3-dichloro-5,6-dicyano-1,4-benzoquinone (DDQ) and boron trifluoride diethyl etherate ($BF_3{\cdot}O(Et)_2$) treatment (Scheme 2). Along with the synthesis of the known PHTT_CHO polymer, this method also employed a metal-free synthetic procedure. The result of these methods allowed for the entirety of the target material PHTT_BDP to be produced in the absence of metals. The scheme and structure of each intermediate is presented in the ESI.

View Article Online
DOI: 10.1039/C6PY01393G

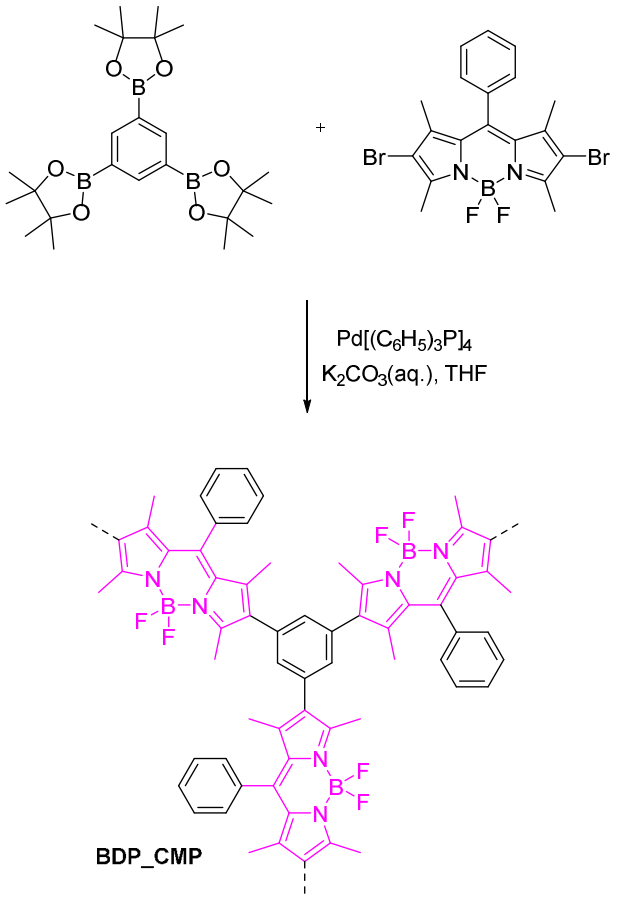

Scheme 1 Synthesis and proposed structure of BDP_CMP.

2,6-diphenyl-1,3,5,7-tetramethyl-8-phenyl-BODIPY (BDP_Ph). To a dry 100 mL-flask equipped with a magnetic stirring bar, a septum inlet, and a reflux condenser was placed a mixture of $Pd[(C_6H_5)_3P]_4$ (5 mg, 0.003 mmol), 2,6-dibromo-1,3,5,7-tetramethyl-8-phenyl-BODIPY (50 mg, 0.10 mmol) and phenylboronic acid (24 mg, 0.20 mmol). This flask was connected to a Schlenk line, evacuated and back-filled with N_2 three times for purging. In the flask, whilst under N_2 dry THF (15 mL) was added to dissolve the reagents. An aqueous solution was prepared with K_2CO_3 (55 mg, 0.4 mmol) and degassed with nitrogen for 10 minutes. The aqueous solution was added through a syringe and the solution was heated to 70°C and stirred overnight. After 16 h, the bright orange reaction mixture was allowed to cool to room temperature before adding approximately 40 mL of water and transferring to a separating funnel with 50 mL of dichloromethane. The organic layer was washed with deionised water (50 mL x 3) and dried over $MgSO_4$. The crude mixture was filtered and a short column using silica gel was used to remove excess catalyst and by-products. Bright orange crystals precipitated from the solution which were filtered, washed with small amount of cold acetone and allowed to dry in air (30 mg, yield: 63%). ^{1}H NMR (300 MHz, $CDCl_3$): δ 7.54-7.49 (m, 3H), 7.44-7.36 (m, 8H), 7.21 (t, 2H), 7.18 (t, 2H), 2.58 (s, 6H), 1.34 (s, 6H).

BDP_CMP. To a dry 100 mL-flask equipped with a magnetic stirring bar, a septum inlet, and a reflux condenser was placed a mixture of $Pd[(C_6H_5)_3P]_4$ (30 mg, 0.03 mmol), 2,6-dibromo-1,3,5,7-tetramethyl-8-phenyl-BODIPY (248 mg, 0.51 mmol) and 1,3,5-tris(4,4,5,5-tetramethyl-1,3,2-dioxaborolan-2-yl)benzene (160 mg, 0.34 mmol). This flask was connected to a Schlenk line, evacuated and back-filled with N_2 three times. In the flask whilst under N_2 dry THF (40 mL) was added to dissolve the solid reagents. An aqueous solution was then prepared with K_2CO_3 (181 mg, 1.03 mmol) and degassed with nitrogen for 10 minutes. The aqueous solution was added to the organic solution, heated to 70°C and stirred overnight. After refluxing for 24 h, a precipitate formed and was filtered and washed three times with MeOH, THF and H_2O. The precipitate was purified *via* soxhlet extraction with THF and $CHCl_3$ for 4 h. The solid reddish powder was dried for 24 h *in vacuo* (176 mg, yield: 72.5%). ^{13}C NMR CP-MAS (100.6 MHz): δ 155.0, 142.0, 134.6, 131.3, 128.5, 12.53.

PHTT_DMP (Step 1). PHTT_CHO (102 mg, 0.17 mmol) and a stir bar were loaded into a 5-mL Schlenk tube. The Schlenk tube was connected to a Schlenk line, evacuated and back-filled with N_2 three times for purging. 2,4-Dimethylpyrrole (1.43 g, 15 mmol, bubbled with N_2 for 5 min beforehand) was transferred into the tube *via* cannula. Trifluoroacetic acid (TFA) (2 drops) was then added into the reaction mixture under N_2. After the mixture was stirred at 50 °C for one day, a brown red solid was collected on a Buchner funnel after the reaction mixture was cooled down to the room temperature, washed with Na_2CO_3/DI water solution, deionised water (10 mL × 4, pH~7), MeOH (10 mL × 2), DCM (10 mL) and dried under vacuum at room temperature for 3 h to afford the as-made product PHTT_DMP as brown-red solid (152 mg). The crude product was purified *via* Soxhlet extraction in refluxing MeOH for 48 h, and then

View Article Online
DOI: 10.1039/C6PY01393G

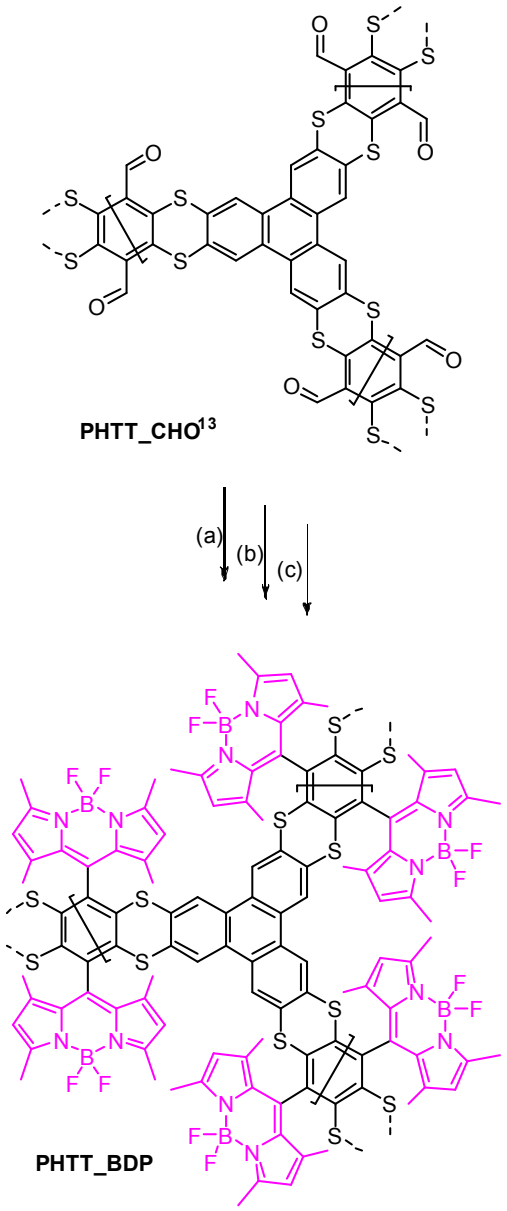

Scheme 2 Synthesis and proposed structure of PHTT_BDP. Reactions conditions: (a) Dimethylpyrrole, 50 °C, TFA. (b) DDQ, DCM, r.t. (c) Trieyhtleamine, $BF_3{\cdot}O(Et)_2$, DCM, 50 °C.

evacuated by pump at 50 °C for 5 h to provide an activated solid product PHTT_DMP (brown-red solid, 145 mg, yield: 76.9%). ^{13}C NMR CP-MAS (100.6 MHz): δ 135.0, 128.6, 110.1, 11.31.

PHTT_DMP_O (Step 2). PHTT_DMP (120 mg, 0.11 mmol), 2,3-dichloro-5,6-dicyano-1,4-benzoquinone (DDQ) (110 mg, 0.48 mmol) and dry DCM (5 mL) were added into a 7.5 mL glass vial. The reaction mixture was stirred at room temperature for 24 h. The black-brown solid was then collected on a Buchner funnel, washed with DCM (10 mL x 3) and dried under vacuum at room temperature for 5 h to afford the product PHTT_DMP_O (115 mg) as a black-brown solid. ^{13}C NMR CP-MAS (100.6 MHz): δ 130.39 (broad 110 – 140), 15.22.

PHTT_BDP (Step 3). PHTT_DMP_O (110 mg, 0.10 mmol) and a stir bar were loaded into a 10 mL Schlenk tube. The Schlenk tube was connected to a Schlenk line, evacuated and back-filled with N_2 three times for purging. Triethylamine (320 mg, 3.2 mmol) in dry DCM (2 mL) (bubbled with N_2 for 2 minutes beforehand) was transferred into the flask via cannula. After the reaction mixture was stirred at room temperature for 10 minutes, $BF_3{\cdot}O(Et)_2$ (670 mg, 4.72 mmol) was added into the reaction mixture under nitrogen protection. The reaction mixture was then stirred at 50 °C for 24 h. The black-brown solid was collected on a Buchner funnel, washed with DCM (10 mL × 5) and dried under vacuum at room temperature for 5 h to afford the product PHTT_BDP (116 mg) as black-brown solid. ^{13}C NMR CP-MAS (100.6 MHz): δ 149.9, 138.4, 129.7, 124.5, 14.20.

Photosensitisation reactions

General procedure and experimental conditions for photosensitisation reactions in flow are exemplified as follows: BDP_CMP (5 mg) was dispersed into a solution containing $CHCl_3$ (15 mL) and α-terpinene (136 mg, 1 mmol). This dispersion (ESI Fig. S1-right) was then pumped using a peristaltic pump through the commercial photochemical reactor employing 1 mm I.D. PTFE tubing at a flow rate of 1 mL min^{-1}. Concurrently, air was pumped through a second pump at the same flow rate. In order to simplify the experimental set-up we chose to use air rather than pure oxygen. The use of two peristaltic pumps allowed for (i) a heterogeneous mixture to pass easily through the system and (ii) air to be pumped through the reactor coil. The dispersion and the air were mixed through a T-junction prior entering to the photochemical coil reactor (10 mL total volume) equipped with a 530 nm LED module. The LED module contains six small arrays and sits in the middle of the coil reactor to ensure full irradiation of the photochemical reactor.[36] This mixture was cycled through several times until full conversion was observed.

Due to the risk of polymer agglomeration and consequent blockage, care was taken to minimise this issue. The polymers were ground into a fine powder before dispersal in solvent, ensuring that the particles are small enough to travel uninhibited through the 1 mm I.D. of the tubing as well as aiding in an even dispersion in each of the solvents tested. A magnetic stirrer was also used to ensure that the dispersion was uniform throughout the experiment. Employing a minimal amount of the photoactive polymer to the reaction mixtures also ensured an appropriately dilute dispersion and further reduced the risk of blockages. It is noted that the dispersion did not increase the flow pressure throughout the experiment indicating that any viscosity increase was negligible.

Results and Discussion

Spectroscopic Properties

View Article Online
DOI: 10.1039/C6PY01393G

The solid-state UV-Vis. absorption spectra of BDP_CMP shows a maximum at 550 nm (ESI Fig. S9). Interestingly, the intermediate steps between PHTT_CHO and PHTT_BDP present with increased broadening of the absorption wavelength and a more intense absorbance between 500-600 nm. The absorbance reaches a peak with the PHTT_BDP product developing a pronounced λ_{max} at 520 nm (ESI Fig. S11). These materials are slightly red-shifted in comparison with the synthesised 1,3,5,7-tetramethyl-8-phenyl-BODIPY monomer, which has an absorption maximum at around 500 nm.[39] This red-shift occurs due to the enhanced delocalisation of the electrons in the polymer.[9, 42]

Since the BODIPY-based polymers mainly absorb light at a lower energetic region of the electromagnetic spectrum chances of photodecomposition of the material and/or reagents are in principle greatly reduced. The absorption edges of both polymers at approximately 700 nm allows for the optical band-gap to be approximately calculated according to the Planck-Einstein relation as shown in Eq. (1):

$$Eg_{(opt.)} = h\frac{c}{\lambda} \quad (1)$$

where $Eg_{(opt.)}$ (J) is the optical band-gap of the polymer, h being the Planck constant (6.63 x 10-34 Js), c the speed of light in vacuum (3.00 x 108 m s^{-1}), and λ being the wavelength (m) at the absorption edge. With an absorption edge at 700 nm, the optical band-gap of both polymers thus calculated equates to 1.77 eV (1 eV = 1.60 x 10^{-19} J). This is not surprising as BODIPY derivatives exhibit variable redox chemistry, and they have been used as electron donors and acceptors.[43, 44] In the latter case, BODIPY co-monomers have the potential of lowering the band gap of conjugated polymers (and stabilising their reduced states), since donor and acceptor units within conjugated structures are able to bring the HOMO/LUMO energy levels closer together.[45, 46]

Absorption and fluorescence spectra of BDP_CMP and its monomeric version Ph_BDP can be in Fig. S10. Both materials were examined first using UV-Vis absorption measurements to determine the maximum absorption wavelengths. BDP_CMP and Ph_BDP presented with a λ_{max} at 520 nm and 527 nm, respectively. We note that due to the insoluble nature of BDP_CMP, it was suspended in CH_2Cl_2 for both the absorption and fluorescence measurements. Excitation at these wavelengths presented with sharp emission spectra showing a weakly Stokes-shifted band of mirror image shape when compared to the absorption spectra. A red shift of both BDP_CMP and Ph_BDP absorption and emission spectra presented with a maximum at 541 and 551 nm, respectively. This can be attributed to the extended π conjugation, particularly in BDP_CMP. Similar characterisation was also performed on PHTT_BDP but no fluorescence was observed.

FT-IR measurements of BDP_CMP were compared to that of the 1,3,5,7-tetramethyl-8-phenyl-BODIPY small molecule (ESI Fig. S12). A characteristic peak at ~1700 cm^{-1} pertaining to a C=N stretch can be seen in both spectra, indicating the presence of the BODIPY moiety within the polymer. PHTT_BDP was also measured *via* FT-IR and compared against the three preceding steps (ESI Fig. S13). The characteristic aldehyde stretch at 1700 cm^{-1} is seen in the initial polymer PHTT_CHO. However, the addition of pyrroles to the aldehyde functionality was supported by the regression of this peak.

Solid-state ^{13}C NMR CP-MAS was also employed to BDP_CMP and PHTT_BDP along with the PHTT_DMP and PHTT_DMP_O intermediates (ESI Fig. S5-8). BDP_CMP presented primarily with aromatic carbons between 142-128 ppm with a smaller signal at 155 which was attributed to the C=N bonds. A signal at 12.5 ppm was also seen, indicating the presence of CH_3 groups. Data for PHTT_BDP and the intermediates was difficult to differentiate, as much of the structures distinctive functional groups are not affected throughout the synthesis. Each showed grouping of broad signals in the 110 – 150 ppm range which can be attributed to large quantity of aromatic carbons in all of these materials. However, the appearance of signals at 11.3, 15.22 and 14.2 ppm for PHTT_DMP, PHTT_DMP_O and PHTT_BDP, respectively, indicates the presence of CH_3 groups found on the dimethylpyrrole groups. The disappearance of the aldehyde signal also indicates the pyrrole groups have replaced this functional group, thus confirming the addition of dimethylpyrrole to PHTT_CHO was successful.

Physical and Thermal Analysis

Considerable porosity of the BODIPY-based and intermediate polymers was seen in both N_2 sorption (at 77 K, ESI Fig. S18-25) and CO_2 sorption (at 273 K, ESI Fig. S26-33) experiments. Typical type-I N_2 adsorption isotherms were observed, with BET measurements showing relatively high surface areas of 769 m^2 g^{-1} for BDP_CMP and 484 m^2 g^{-1} for PHTT_BDP, which is in line with most reported CMPs.[9] QSDFT analysis on pore size distribution and pore volume indicated for BDP_CMP an average pore width of 0.545 nm and pore volume of 0.563 cm^3 g^{-1} and for PHTT_CMP an average pore width of 1.096 nm and pore volume of 0.523 cm^3 g^{-1}. Interestingly, an increase in pore volume was observed from 0.374 cm^3 g^{-1} for PHTT_CHO to 0.448 cm^3 g^{-1} for PHTT_DMP_O and finally to 0.523 cm^3 g^{-1} for PHTT_BDP. A summary of surface area and pore size/volume values for all synthesised polymers can be found in Table S2.

Since the BODIPY moiety was grafted onto PHTT_CHO post-synthetically, it is worth noting the decrease in surface area from 686 m^2 g^{-1} for the aldehyde-equipped precursor to 484 m^2 g^{-1}.[13] This is not surprising given that BODIPY is a bulky molecule that contributes to the decrease in surface area and as expected is also observed in the intermediate polymers. Nevertheless, both materials present high surface areas and we have previously demonstrated the importance of surface area in photocatalytic processes.[11] In general as surface area of the photocatalyst increases, the interface between the polymeric material and the medium also increases, thus resulting in greater photocatalytic efficiencies. Both BODIPY-based CMPs, in this instance, fulfil the requirements for an efficient photosensitiser for the production of $^1O_2$.

TGA for all products was also performed. TGA for BDP_CMP (ESI Fig. S14) showed good thermal stability up to

View Article Online
DOI: 10.1039/C6PY01393G

300 °C and with 40% weight percentage remaining at 950 °C. TGA measurements of PHTT_BDP and its intermediates (ESI Fig. S15-17) also showed high thermal stability up to 300 °C. When compared to the PHTT_CHO starting material,[13] decreased thermal stability at higher temperatures is observed in the intermediate products while the final PHTT_BDP product regains some of this stability. When comparing to BDP_CMP, at 950 °C only 20% weight percent of the product remained, exhibiting PHTT_BDP as the less stable of the two BODIPY-based polymers at elevated temperatures.

SEM and TEM images (ESI Fig. S34-41) established the target polymers as highly textured, amorphous surfaces, indicating the potential for high surface areas. EDX analysis (ESI Fig. S42-45) demonstrates the primary difference between the two BODIPY-based polymers and their respective synthetic methods. While the Pd catalysed Suzuki cross-coupling reaction presents with minute traces of Pd metal (0.94 wt.%) remaining within the polymer matrix, the metal-free synthetic procedure clearly shows no presence of trace metal species.

Heterogeneous Photosensitisation at 530 nm

Using the BODIPY-based CMPs as heterogeneous photosensitisers, $^1O_2$ production was carried out in a commercial photochemical flow reactor equipped with an LED module with narrow emission at 530 nm (easy-Photochem from Vapourtec, Fig. S2) as described above. The setup used is illustrated in the schematic diagram in Fig. 2.

The progress of the Alder-ene reaction (Scheme 3) was followed by ^{1}H NMR spectroscopy, and the conversion calculated from the ratio of peaks assigned to the starting material (α-terpinene) and the product (ascaridole) (ESI Fig. S3). This Alder-ene reaction was chosen as it is well-established that α-terpinene is extremely susceptible to photosensitised $^1O_2$

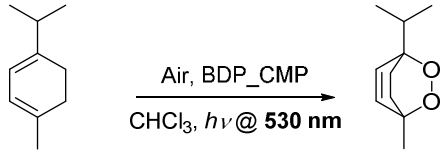

Scheme 3 Synthesis of ascaridole from α-terpinene *via* the photosensitisation of $^1O_2$ under green light irradiation.

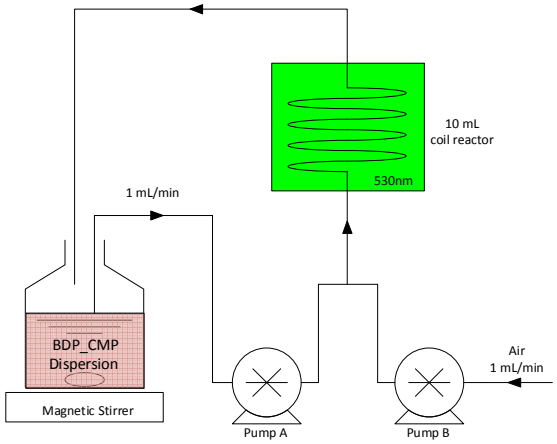

Fig. 2 Schematic representation of the experimental set-up using the easy-Photochem flow reactor from Vapourtec.

oxidation while being rather stable against other oxidants such as ozone (O_3), hydrogen peroxide (H_2O_2) and hydroxyl radical ($OH^{\bullet}$).[47, 48]

After a 1 h period, both the BDP_CMP and PHTT_BDP polymers were able to fully convert (>99%) α-terpinene into ascaridole in chloroform. This confirms that both materials can act as photosensitisers for the production of $^1O_2$. In order to further verify the photostability of the BODIPY-based CMPs and

using the same conditions as described above (of light and air), we cycled in the absence of α-terpinene a new dispersion for 5 hours after which α-terpinene (136 mg, 1 mmol) was added. The dispersion was then cycled through the photochemical reactor for another 60 min. Samples were taken every 10 min and the conversions were calculated and plotted (Fig. 3). The tabulated values can be found in the ESI Table S1.

BDP_CMP shows enhanced photostability when compared to PHTT_BDP. This may be attributed to the fact that within BDP_CMP the BODIPY moiety is an integral part of the backbone of the polymer repeat unit whereas PHTT_BDP has the BODIPY grafted onto the polymer backbone without benzene ring attached to it. This may contribute to an enhanced photobleaching of the BODIPY core. Nevertheless, and given that $^1O_2$ was produced during the initial 5 hour-experiment, we also demonstrate that the BDP_CMP polymer is not affected by this powerful oxidant whereas for PHTT_BDP we observed a loss of 10% in its photoactivity. Slight deviations to the initial results can be attributed to experimental error associated to ^{1}H NMR integrations and/or due to the fact that more air was dissolved in the latter experiment since it was aerated for 5 consecutive hours.

The photochemical reaction between $^1O_2$ and the substrate, in this case α-terpinene, is essentially a second-order reaction, where the rate of the reaction is dependent on the concentration of both reactants. However, most studies conducting these photochemical reactions do so under batch conditions where the concentration of the substrate is much greater than the concentration of $^1O_2$. Therefore, the kinetics of

View Article Online
DOI: 10.1039/C6PY01393G

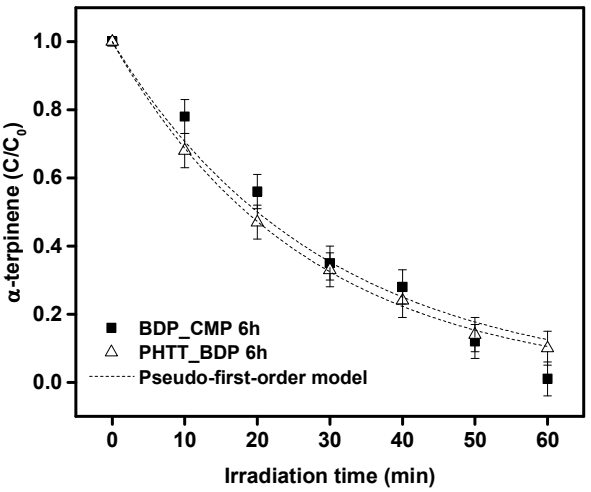

Fig. 3 Conversion of α-terpinene to ascaridole *via* BDP_CMP and PHTT_BDP in chloroform after 6h irradiation at 530 nm. Curves represent non-linear regression fits to the pseudo-first-order model. Error bars indicate potential error in ^{1}H NMR integration values.

reactions between $^1O_2$ and the substrate can be simplified by the pseudo-first-order model.[49-51] This model is expressed as Eq. (2):

$$-\frac{dC}{dt} = kC \quad (2)$$

where C is the concentration of substrate (mM or mg/L), t is the reaction time (h), and k is the pseudo-first-order rate constant (h^{-1}). If the initial concentration of substrate is C_0, Eq. (2) can be integrated as follows:

$$\ln C - \ln C_0 = -kt \quad (3)$$

Eq. (3) can be further presented in exponential form as follows:

$$\frac{C}{C_0} = e^{-kt} \quad (4)$$

The kinetics of α-terpinene conversion were fitted to the pseudo-first-order model by non-linear regression of concentration versus time data for the 6 h experiments (Fig. 3). Results show that the conversion of α-terpinene generally followed this model. However, for the BDP_CMP, conversion near the 60 min mark was greater than expected based on the pseudo-first-order model. This may be explained by the continuous addition of air (and therefore oxygen) being supplied to the flow reactor, leading to a continuous generation of $^1O_2$. At this point in the reaction, the concentration of $^1O_2$ is much greater than that of α-terpinene, hereby not fulfilling the pseudo-first-order model any longer. Therefore, with actual conversion higher than that of the model, a major advantage is highlighted of the continuous flow reaction over the batch method.

Controls and validation of BODIPY

A control experiment was performed under similar conditions using visible light at 420 nm as the source of photons. After 90 minutes, only 9% conversion of α-terpinene into ascaridole was observed, demonstrating the essential need for a light source at 530 nm, which is more suitable for application in photochemical reactions where reagents and/or products are susceptible to photodecomposition at more energetic wavelengths.

Validation of the BODIPY core as the photoactive component within these polymers was performed by employing the synthesised BDP_Ph monomer and testing under the same conditions as the polymeric counterparts. After both 1 hour and 6 hours, full conversion of α-terpinene into ascaridole was observed with no apparent degradation of the monomer, demonstrating the BODIPY core as the essential photoactive component.

To ensure the post modification of PHTT_CHO to PHTT_BDP was required to perform as a photosensitiser at 530 nm, all intermediates of PHTT_BDP were isolated and employed under the same experimental conditions. Table 1 shows the intermediate material conversion values after 1h and how they compare to the other BODIPY-containing materials synthesised. Only a 77% conversion of α-terpinene into ascaridole was observed for the PHTT_DMP and PHTT_DMP_O intermediates while PHTT_BDP showed 100% conversion. While the addition of pyrrole groups to PHTT_CHO demonstrated good photoactivity, this is not surprising as this modification resulted in an increased absorbance at 530 nm. Despite this, only the PHTT_BDP polymer was able to achieve full conversion after 60 minutes thereby validating the addition of the BODIPY core to PHTT_CHO.

Photosensitisation reactions in different solvents

To verify the versatility of the BODIPY-based CMPs in the production of $^1O_2$, different solvents were tested with the same experimental set-up. Life-time of $^1O_2$ varies considerably in different solvents and it is not surprising that some solvents are in effect better than others to perform $^1O_2$ reactions.[47] Nevertheless, and due to different solvation requirements for given substrates, having a wide range of solvents in which $^1O_2$ can be produced heterogeneously further validates the BODIPY-based CMPs as universal $^1O_2$ photosensitisers in a variety of organic transformations. Commonly used organic solvents that were tested in this study, along with the corresponding lifetime of $^1O_2$ in the respective solvents, are tabulated in Table 2. In general, as the lifetime of $^1O_2$ in a solvent decreases, the percent conversion of α-terpinene to ascaridole also declines. Ethanol presents as the one slight outlier, showing an enhanced conversion when comparing to the $^1O_2$ lifetime in this solvent. Water was also tested in the same conditions, however, due to the hydrophobicity of both CMPs, a uniform dispersion was not achievable and polymer aggregates were observed, which

View Article Online
DOI: 10.1039/C6PY01393G

Table 1 Conversion of α-terpinene into ascaridole in chloroform after 60 min employing different photosensitisers using the described photochemical reactor

Photosensitiser	Conversion (%)[a]
PHTT_DMP	77
PHTT_DMP_O	77
PHTT_BDP	>99
BDP_Ph	>99
BDP_CMP	>99

[a] Percent conversion calculated from integrated ^{1}H NMR signals.

Table 2 Conversion of α-terpinene into ascaridole in chloroform after 60 min in different solvents using the described photochemical reactor

Solvent	Conv. w/ BDP_CMP (%)[a]	Conv. w/ PHT_BDP (%)[a]	Lifetime (s)[52]
Chloroform	>99	>99	$2.5 \cdot 10^{-4}$
Acetonitrile	98	99	$7.5 \cdot 10^{-5}$
Ethanol	88	92	$1.2 \cdot 10^{-5}$
THF	87	92	$3 \cdot 10^{-5}$
Toluene	85	81[d]	$2.5 \cdot 10^{-5}$
Acetone	83	92	$1.2 \cdot 10^{-5}$
Green Solvents:			
2-Methyl THF	93	81	-[e]
DMC[b]	92	91	-[e]
Water[c]	-	-	$4.2 \cdot 10^{-6}$

[a] Percent conversion calculated from integrated ^{1}H NMR signals. [b] Dimethylcarbonate. [c] Aggregation of BDP_CMP and PHTT_BDP in water impeded the flow process. [d] PHTT_BDP dispersed poorly in toluene, impeding flow of the photosensitiser and therefore decreasing potential for $^1O_2$ generation. [e] No available data.

invariably led to the blockage of the flow reactor. Since water is a "green" solvent, two other solvents under the same classification, dimethylcarbonate (DMC) and 2-methyltetrahydrofuran (2-MeTHF) were also tested. These exhibited comparable results to those of the commonly used organic solvents, demonstrating their potential to replace more environmentally harmful solvent systems.

DMC and 2-MeTHF can be classed as green solvents as they are derived from renewable resources such as biomass rather than petroleum. DMC is attractive as an alternative solvent because it can be produced by the catalytic oxidative carbonylation of methanol, a method that avoids the use of toxic phosgene.[53] Furthermore, in 2009 DMC was made exempt under the definition of volatile organic compounds (VOCs) by the United States Environmental Protection Agency.[54] 2-MeTHF can be obtained from agricultural by-products and has been shown to give good results in a variety of synthetic process, having already been applied in industry.[55]

Conclusions

In conclusion, BODIPY-based conjugated microporous polymers with high surface areas (484-769 $m^2\ g^{-1}$) have been prepared by two distinct methods: direct assembly *via* a palladium-catalysed Suzuki-Miyaura cross-coupling reaction and a post-synthetic transformation of an aldehyde-equipped CMP host that overall was synthesised in the absence of metals. Employing a strategy whereby a strong electron acceptor (BODIPY) is coupled to weak electron donors (benzene), we were able to bathochromically shift the maximum absorbance of the CMPs towards a less energetic wavelength (530 nm) of the visible spectrum. The polymer products were then tested in a commercial photochemical flow reactor (Vapourtec Ltd) equipped with an LED module at 530 nm as the source of photons for the production of $^1O_2$ in a variety of solvents. $^1O_2$ production was monitored *via* ^{1}H NMR *via* the conversion of α-terpinene into ascaridole. Overall, the polymers demonstrated high photostability, especially with BDP_CMP showing no loss in photoactivity. These materials were easily recoverable *via* simple filtration and reused for further $^1O_2$ reactions. This work shows that conjugated porous polymers represent a new promising family of recyclable heterogeneous photocatalysts, with tuneable light absorption and which will significantly simplify the handling and purification of sensitive reactions, presenting itself as a more sustainable class of materials that potentially can be applied to different photocatalytic processes.

Moreover, the successful deployment of the above two synthetic schemes points to a number of broad-scope advantages. First, the robust aryl-aryl links of the BDP_CMP backbone provides outstanding compatibility and stability properties (e.g., compared with the more fragile and reactive alkyne-based link) for real-world applications. Such stability is well illustrated in the above extensive investigations on photochemical catalysis properties, wherein highly reactive species (e.g., $^1O_2$) is constantly being generated, and long-term stability of the host backbone is crucial for reusable, sustainable applications. Second, the post-synthetic approach for preparing PHTT_BDP involves no transition or heavy metal reagents at any step, and thus minimises health and environmental concerns. Moreover, the post-synthetic transformation of the aldehyde groups offers functional flexibility. For example and in future work, the dipyrrin precursor can chelate to metal centres other than the boron unit, and thereby imparting onto the CMP backbone the diverse and versatile reactivities of metal-dipyrrin complexes.

Acknowledgements

We would like to acknowledge Vapourtec Ltd. for their valuable technical support. F. Vilela would like to thank Heriot-Watt University and The Royal Society for financial support (**RG140169)**. M. Demleitner would like to thank the ERASMUS programme for financial support. X. Zu would like to thank the Research Grants Council of HKSAR for financial support (**City U 11303414**).

Notes and references

1 N. B. McKeown and P. M. Budd, *Chem. Soc. Rev.*, 2006, **35**, 675-683.
2 J. Germain, J. M. J. Frechet and F. Svec, *Small*, 2009, **5**, 1098-1111.

View Article Online
DOI: 10.1039/C6PY01393G

3 R. S. Sprick, J.-X Jiang, B. Bonillo, S. Ren, T. Ratvijitvech, P. Guiglion, M. A. Zwijnenburg, D. J. Adams and A. I. Cooper, *J. Am. Chem. Soc.*, 2015, **137**, 3265-3270.
4 F. Vilela, K. Zhang and M. Antonietti, *Energy Environ. Sci.*, 2012, **5**, 7819-7832.
5 J.-X. Jiang, F. Su, A. Trewin, C. D. Wood, N. L. Campbell, H. Niu, C. Dickinson, A. Y. Ganin, M. J. Rosseinsky, Y. Z. Khimyak, and A. I. Cooper, *Angew. Chem. Int. Ed.*, 2007, **46**, 8574-8578.
6 J. X. Jiang, C. Wang, A. Laybourn, T. Hasell, R. Clowes, Y. Z. Khimyak, J. Xiao, S. J. Higgins, D. J. Adams and A. I. Cooper, *Angew. Chem. Int. Ed.*, 2011, **50**, 1072-1075.
7 J.-X. Jiang and A. Cooper, *Top. Curr. Chem.*, 2010, **293**, 1-33.
8 X. Liu, S. A, Y. Zhang, X. Luo, H. Xia, H. Li and Y. Mu, *RSC Adv.*, 2014, **4**, 6447-6453.
9 Y. Xu, S. Jin, H. Xu, A. Nagai and D. Jiang, *Chem. Soc. Rev.*, 2013, **42**, 8012-8031.
10 J.-X. Jiang, Y. Li, X. Wu, J. Xiao, D. J. Adams and A. I. Cooper, *Macromol.*, 2013, **46**, 8779-8783.
11 K. Zhang, D. Kopetzki, P. H. Seeberger, M. Antonietti and F. Vilela, *Angew. Chem. Int. Ed.*, 2013, **52**, 1432-1436.
12 J. Liu, J. M. Tobin, Z. Xu and F. Vilela, *Polym. Chem.*, 2015, **6**, 7251-7255.
13 J. Liu, J. Cui, F. Vilela, J. He, M. Zeller, A. D. Hunter and Z. Xu, *Chem. Commun.*, 2015, **51**, 12197-12200.
14 K. Zhang, Z. Vobecka, K. Tauer, M. Antonietti and F. Vilela, *Chem. Commun.*, 2013, **49**, 11158-11160.
15 H. Urakami, K. Zhang and F. Vilela, *Chem. Commun.*, 2013, **49**, 2353-2355.
16 G. Herzberg, *Molecular Spectra and Molecular Structure I: Spectra of Diatomic Molecules*; 2nd Ed. VonNostrand, New York, 1950.
17 T. Nyokong and V. Ahsen, *Photosensitizers in Medicine, Environment and Security*; Springer, London, 2012.
18 M. C. DeRosa and R. J. Crutchley, *Coord. Chem. Rev.*, 2002, **233-234**, 351-371.
19 E. L. Clennan, *Tetrahedron*, 2000, **56**, 9151-9179.
20 J. Shen, R. Steinbach, J. M. Tobin, M. M. Nakata, M. Bower, M. R. S. McCoustra, H. Bridle, V. Arrighi and F. Vilela, *Appl. Cat. B – Enviorn.*, 2016, **193**, 226-233.
21 R. Bonnett, *Chem. Soc. Rev.*, 1995, **24**, 19-33.
22 S. O. McDonnell, M.J. Hall, L. T. Allen, A. Byrne, W. M. Gallagher and D. F. O'Shea, *J. Am. Chem. Soc.*, 2005, **127**, 16360-16361.
23 A. Loudet and K. Burgess, *Chem. Rev.*, 2007, **107**, 4891-4932.
24 G. Ulrich, R. Ziessel and A. Harriman, *New J. Chem.*, 2007, **31**, 496-501.
25 G. Ulrich, R. Ziessel and A. Harriman, *Angew. Chem. Int. Ed.*, 2008, **47**, 1184-1201.
26 Q. D. Zheng, G. X. Xu and P. N. Prasad, *Chem.-Eur. J.*, 2008, **14**, 5812-5819.
27 Y. Ikawa, S. Moriyama and H. Furuta, *Anal. Biochem.*, 2008, **378**, 166-170.
28 M. A. H. Alamiry, A. C. Benniston, G. Copley, K. J. Elliott, A. Harriman, B. Stewart and Y. G. Zhi, Dye. *Chem. Mater.*, 2008, **20**, 4024-4032.
29 O. Garcia, L. Garrido, R. Sastre, A. Costela and I. Garcia-Moreno, *Adv. Funct. Mater.*, 2008, **18**, 2017-2025.
30 A. Costela, I. Garcia-Moreno, M. Pintado-Sierra, M. Amat-Guerri, M. Liras, R. Sastre, F. L. Arbeloa, J. B. Prieto and I. L. Arbeloa, *J. Photochem. Photobiol. A*, 2008, **198**, 192-198.
31 S. Mula, A. K. Ray, M. Banerjee, T. Chaudhuri, K. Dasgupta and S. Chattopadhyay, *J. Org. Chem.*, 2008, **73**, 2146-2154.
32 S. Erten-Ela, M. D. Yilmaz, B. Icli, B. Y. Dede, S. Icli and E. U. Akkaya, *Org. Lett.*, 2008, **10**, 3299-3302.
33 L. Bonardi, H. Kanaan, F. Camerel, P. Jolinat, P. Retailleau and R. Ziessel, *Adv. Funct. Mater.*, 2008, **18**, 401-413.
34 M. M. Sartin, F. Camerel, A. J. Ziessel and J. Bard, *J. Phys. Chem. C*, 2008, **112**, 10833-10841.
35 S. G. Awuah and Y. You, *RSC Adv.*, 2012, **2**, 11169-11183.
36 Vapourtec, http://www.vapourtec.co.uk/, accessed August 2016.
37 M. Ranger, D. Rondeau and M. Leclerc, *Macromolecules*, 1997, **30**, 7686-7691.
38 P. V. Dau, K. K. Tanabe and S. M. Cohen, *Chem. Commun.*, 2012, **48**, 9370-9372.
39 A. Vazquez-Romero, N. Kielland, M. J. Arevalo, S. Preciado, R. J. Mellanby, Y. Feng, R. Lavilla and M. Vendrell, *J. Am. Chem. Soc.*, 2013, **135**, 16018-16021.
40 L. Wang, J-W. Wang, A-j, Cui, X-X. Cai, Y. Wan, Q. Chen, M-Y. He and W. Zhang, *RSC Adv.*, 2013, **3**, 9219-9222.
41 Y. Chen, J. Zhao, H. Guo and L. Xie, *J. Org. Chem.*, 2012, **77**, 2192-2206.
42 M. Liras, M. Iglesias and F. Sanchez, *Macromol.*, 2016, **49**, 1666-1673.
43 M. D. Yilmaz, O. A. Bozdemir and E. U. Akkaya, *Org. Lett.*, 2006, **8**, 2871-2873.
44 R. Ziessel, C. Goze, G. Ulrich, M. Cesario, P. Retailleau, A. Harriman and J. P. Rostron, *Chem.–Eur. J.*, 2005, **11**, 7366-7378.
45 J. C. Forgie, P. J. Skabara, I. Stibor, F. Vilela and Z. Vobecka, *Chem. Mat.*, 2009, **21**, 1784-1786.
46 D. C.-Lacalle, C. T. Howells, S. Gambino, F. Vilela, Z. Vobecka, N. J. Findlay, A. R. Inigo, S. A. J. Thomson, P. J. Skabara and I. D. W. Samuel, *J. Mater. Chem.*, 2012, **22**, 14119-14126.
47 S. Ogawa, S. Fukui, Y. Hanasaki, K. Asano, H. Uegaki, F. Sumiko and S. Ryosuke, *Chemosphere*, 1991, **22**, 1211-1225.
48 D. Choi and M. Jung, *Food Sci. Biotechnol.*, 2013, **22**, 249-256.
49 H. Kim, W. Kim, Y. Mackeyev, G.-S. Lee, H.-J. Kim, T. Tachikawa, S. Hong, S. Lee, J. Kim, L. J. Wilson, T. Majima, P. J. J. Alvarez, W. Choi and J. Lee, *Environ. Sci. Technol.*, 2012, **46**, 9606–9613.
50 T. Zhang, Y. Ding and H. Tang, *Chem. Eng. J.*, 2015, **264**, 681–689.
51 J. Lee, Y. Mackeyev, M. Cho, L. J. Wilson, J.-H. Kim and P. J. J. Alvarez, *Environ. Sci. Technol.,* 2010, **44**, 9488–9495.
52 F. Wilkinson, W. P. Helman and A. B. Ross, *J. Phys. Chem. Ref. Data*, 1995, **24**, 663-1021.
53 L. Rossi, S. Grego, A. E. Rosamilia, F. Arico and P. Tundo, *Green Chemical Reactions*, Springer Link, 2008, 213-232.
54 US-EPA, https://www3.epa.gov/ttn/oarpg/t1pfpr.html, Accessed August 2016.
55 V. Antonucci, J. Coleman, J. B. Ferry, N. Johnson, M. Mathe, J. P. Scott and J. Xu, *Org. Process Res. Dev.*, 2011, **15**, 939-941.

View Article Online
DOI: 10.1039/C6PY01393G

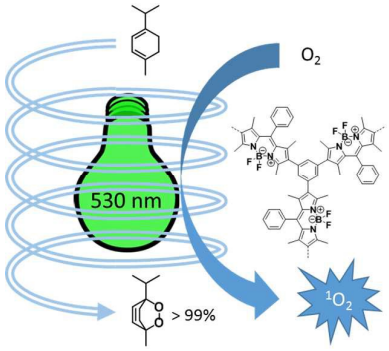

Production of singlet oxygen at 530 nm in flow using novel BODIPY-based polymers as heterogeneous photosensitisers